IEEE Access
Multidisciplinary | Rapid Review | Open Access Journal

Received January 10, 2019, accepted January 30, 2019, date of publication February 1, 2019, date of current version February 20, 2019.

Digital Object Identifier 10.1109/ACCESS.2019.2897043

A Barrage Noise Jamming Method Based on Double Jammers Against Three Channel SAR GMTI

XIN CHANG AND CHUNXI DONG
School of Electronic Engineering, Xidian University, Xi'an 710071, China

Corresponding author: Chunxi Dong (chxdong@mail.xidian.edu.cn)

This work was supported in part by the National Defense Pre-Research Program during the 12th Five-Year Plan under Grant under Grant 411****0301, and in part by the National Basic Research Program (973 Program) under Grant 61**81.

ABSTRACT Many jamming methods have been proposed against displaced phase center antenna (DPCA) process, which is a type of three-channel synthetic aperture radar (SAR) ground moving target indication. However, two important problems faced by the jammer are why the jamming based on a single jammer is suppressed and how to generate noise in the whole DPCA image while keeping its easy realization. By analyzing a jamming geometric model based on a single jammer, the reason is that the phase of the jamming image in different antennas is only relative to the jamming geometric model, which contains the azimuth position of the jammer and jamming in the SAR image. Then, the jamming area is classified as an enhanced area and a weakened area after DPCA processing. Moreover, the jamming in the weakened area will be suppressed. To overcome this disadvantage, a barrage noise jamming method based on double jammers is proposed. By controlling the azimuth distance between the jammers, the noise can cover the whole DPCA image. Compared with the deception jamming method based on multiple coherent jammers, the phase and amplitude of the jamming signal do not need to be accurately controlled. Finally, the validity of the proposed method is verified by simulation experiments.

INDEX TERMS Synthetic aperture radar (SAR), ground moving target indication (GMTI), displaced phase center antenna (DPCA), barraged jamming, double jammers.

I. INTRODUCTION

Due to capabilities of all-time and high resolution imaging under complex weather condition, synthetic aperture radar (SAR) has been widely applied in both civil and military field to acquire information of the sensitive area [1], [2]. Ground moving target indication (GMTI) has played a vital role in detection, location and imaging of moving targets. Due to easy realization, displaced phase center antenna (DPCA), one type of three channel SAR GMTI and it is derived from SAR, has been widely utilized ranging from traffic monitoring systems and airport surface surveillance [3]–[5]. In order to prevent SAR with DPCA technique from acquiring accurate moving target information, the study on jamming method against SAR GMTI system becomes one of the most important topics in the field of electromagnetic countermeasure. Furthermore, study on jamming method can help identify the weakness of SAR GMTI system and improve it in the future.

In general, jamming methods can be classified as multiple-path and direct-path jamming method based on the different jamming path. Scattered wave jamming, also known as rebound jamming, is one type of multiple-path jamming and can generate a deception scene or large-scale noise [6]–[8]. However, jamming will be suppressed by DPCA processing concerned with distance between jamming and jammer in azimuth. Huang performed noise in the whole DPCA image by retransmitting the intercepted SAR signal with random time-delay [9]. If radar cross section (RCS) of scattered points of ground is low, a very high jamming power is required in this method [10]. Moreover, the direct-path jamming method also can be classified as deception jamming method and

The associate editor coordinating the review of this manuscript and approving it for publication was Mehmet Alper Uslu.

barrage noise jamming method, and they are always based on a single jammer or antenna. For deception jamming, to obtain the jamming signal of false moving targets by utilizing the intercepted SAR signal, the Doppler shift-frequency modulation, time-delay modulation and segment modulation are performed [11]–[15]. However, in order to generate false targets or false scenes which contents a lot of arrayed and false scatterers, high accuracy of SAR GMTI parameters are required and the high computational burden is faced by jammer [16]–[19]. For barrage noise jamming method, jamming signal can generate noise in the whole SAR image and destroy the acquisition information of moving targets while keeping its easy realization. However, the jamming near the jammer in SAR image will be suppressed by DPCA processing. So, an important problem faced by the jammer is why the jamming based on a single jammer is suppressed. By analyzing jamming geometric model based on a single jammer, the reason is that the phase of jamming image in different antenna is only relative to the jamming geometric model which contains the azimuth position of the jammer and jamming in SAR image. Then, azimuth jamming filter is generated by DPCA processing and its center on a single stationary jammer. The jamming image is classified as an enhanced area and a weakened area. So both barrage noise jamming and deception jamming based on a single jammer are suppressed by DPCA processing. The other important problem faced by the SAR GMTI jammer is how to generate jamming in the whole DPCA image. The phase of jamming signal in antennas are controlled to destroy the suppression of SAR GMTI and interferometry synthetic aperture radar (InSAR) by utilizing the multiple coherent stationary jammers [19], [20]. However, because the high accuracy jamming geometric model is hardly acquired, coherent jamming signal is difficult to generate based on multiple jammers. 3-D deceptive interfering method with double jammers is an effective deception jamming method to generate the false scene and confuse InSAR [21]. However, to generated false scene, the high computational burden of the jammer is still required. So, in this paper, we intended to propose a jamming method which can generate jamming to cover the whole DPCA image while keeping its easy realization.

A barrage noise jamming method based on double jammers against three channel SAR GMTI is proposed by changing the jamming geometric model. By controlling the azimuth distance between the double jammers, the jamming can cover the whole SAR and DPCA images and prevent SAR GMTI from acquiring the information of moving targets. Compared with the deception jamming method based on multiple coherent jammers, the phase and amplitude of jamming signal do not need to be accurately controlled. This makes the proposed jamming much easier to be realized. The rest of this paper is organized as follows. The reason why jamming will be suppressed after DPCA processing is detailed analyzed in Section II. The barrage noise jamming method based on multiple jammers are proposed in Section III to overcome disadvantage of jamming method based on a single jammer while keeping its easy realization. In Section IV, simulation results are provide to validate the effectiveness of the proposed method. Section V concludes this paper.

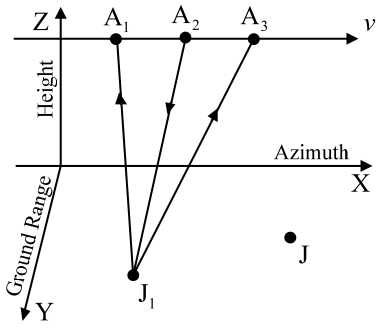

FIGURE 1. Geometric model of jamming based on a single jammer.

II. ANALYSIS OF JAMMING EFFECT BASED ON A SINGLE STATIONARY JAMMER

In this section, jamming effect based on a signal jammer is briefly presented. In addition, the important problem faced by the jammer about why the jamming based on a single jammer is suppressed is analyzed.

As shown in Fig. 1, SAR GMTI is assumed work at boardside mode. The X-axis is the azimuth direction aligned with the SAR GMTI velocity vector, the Y-axis is the ground range direction, and the Z-axis is perpendicular to the ground and represent Height. The platform of SAR GMTI moves at a constant velocity v along the azimuth direction, X-axis, at altitude h.

The SAR GMTI contains three antennas, and these antennas are denoted by the points A_1, A_2, and A_3, respectively. The signal is transmitted from antenna A_2 and is received by antennas A_1 and A_3. Their coordinates are $(vt_aD, 0, h)$, $(vt_a, 0, h)$ and $(vt_a + D, 0, h)$ varying with t_a, where t_a is the slow time and D is the distance among the antennas. D satisfies the DPCA condition that $D = N \bullet v/\mathrm{PRF}$ where N is a positive integer, and PRF is the pulse repetition frequency [10].

A single stationary jammer is denoted by the point J1, and its coordinate is $(x_1, y_1, 0)$.The jamming signal is transmitted by the jammer to SAR GMTI. Although the jamming signal are different based on different method, geometric jamming model is the same. So the following analysis of jamming effect is suitable for the jamming method based on a single jammer, including the barrage noise jamming method and the deception jamming method. Without loss of generality, the deception jammer, which it retransmits the intercepted SAR signal to form the false target, is used in this section, and the process of DPCA is shown in Fig. 2 [3].

The linear frequency modulation (LFM) signal that is transmitted by SAR GMTI system can be described as follows.

$$S_0(t_r, t_a) = a_r(t_r)exp\{\mathrm{j}2\pi\ [f_0(t_r + t_a) + 0.5\gamma t_r^2]\} \quad (1)$$

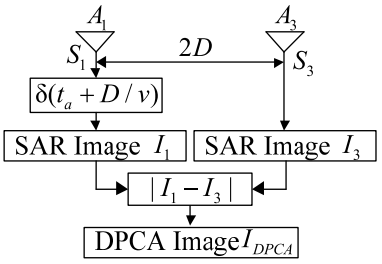

FIGURE 2. The process of DPCA.

where t_r is the fast time, f_0 is the radar center frequency, γ is the chirp rate, and $a_r(t_r) = \begin{cases} 1|t_r| \le T_r/2 \\ 0|t_r| > T_r/2 \end{cases}$ presents pulse envelope of the signal where T_r is the pulse duration.

The distance between the antenna A_2 and the stationary jammer J_1 varying t_a is described as follows.

$$\begin{aligned} R_{A_2J_1}(t_a) &= \sqrt{(vt_a - x_1)^2 + y_1^2 + h^2} \\ &\approx R_1 - \frac{vx_1}{R_1}t_a + \frac{v^2t_a^2}{2R_1} \end{aligned} \tag{2}$$

where $R_1 = \sqrt{x_1^2 + y_1^2 + h^2}$.

Similarly, the distance between the jammer J_1 and the antenna A_1 and that between the jammer J_1 and the antenna A_3 varying t_a, respectively, are described as follows.

$$\begin{aligned} R_{J_1A_1}(t_a) &= \sqrt{(vt_a - D - x_1)^2 + y_1^2 + h^2} \\ &\approx R_{A_2J_1}(t_a) - \frac{vD}{R_1}t_a + \frac{x_1D}{R_1} + \frac{D^2}{2R_1} \end{aligned} \tag{3}$$

$$\begin{aligned} R_{J_1A_3}(t_a) &= \sqrt{(vt_a + D - x_1)^2 + y_1^2 + h^2} \\ &\approx R_{A_2J_1}(t_a) + \frac{vD}{R_1}t_a - \frac{x_1D}{R_1} + \frac{D^2}{2R_1} \end{aligned} \tag{4}$$

The range history of the jammer J_1 for antennas A_1 and A_3, respectively, are summarized as follows:

$$R_{A_1}(t_a) = R_{A_2J_1}(t_a) + R_{J_1A_1}(t_a) \tag{5}$$

$$R_{A_3}(t_a) = R_{A_2J_1}(t_a) + R_{J_1A_3}(t_a) \tag{6}$$

The baseband echo of jamming signal S_1 and S_3 received by antennas A_1 and A_3 can be described as follows.

$$\begin{aligned} &S_1(t_r, t_a) \\ &= \sigma_J a_r\left(t_r - \frac{R_{A_1}(t_a)}{c}\right) a_{az}\left(t_a - \frac{x_1}{v}\right) \\ &\quad \times \exp\left[j\pi\gamma\left(t_r - \frac{R_{A_1}(t_a)}{c}\right)^2\right] \exp\left[-j\frac{2\pi R_{A_1}(t_a)}{\lambda}\right] \end{aligned} \tag{7}$$

$$\begin{aligned} &S_3(t_r, t_a) \\ &= \sigma_J a_r\left(t_r - \frac{R_{A_3}(t_a)}{c}\right) a_{az}\left(t_a - \frac{x_1}{v}\right) \\ &\quad \times \exp\left[j\pi\gamma\left(t_r - \frac{R_{A_3}(t_a)}{c}\right)^2\right] \exp\left[-j\frac{2\pi R_{A_3}(t_a)}{\lambda}\right] \end{aligned} \tag{8}$$

where λ is the wavelength, σ_J is the gain factor of the jammer, $a_{az}(t_a) = \begin{cases} 1|t_a| \le T_a/2 \\ 0|t_a| > T_a/2 \end{cases}$ is the azimuth envelope where T_a is the jammer exposure time. In order to generate the false target J, which its coordinate is $(x_J, y_J, 0)$, the phase modulation and the time delay modulation are performed by utilizing the intercepted SAR signal. Then the baseband echo of jamming signal is received by antennas A_1 and A_3 can be described as follows [14].

$$\begin{aligned} S_1'(t_r, t_a) &= S_1(t_r, t_a) \cdot exp\left\{-\frac{4\pi[R_{A_2J}(t_a) - R_{A_2J_1}(t_a)]}{\lambda}\right\} \\ &\quad * \delta\left\{t_r - \frac{2[R_{A_2J}(t_a) - R_{A_2J_1}(t_a)]}{c}\right\} \end{aligned} \tag{9}$$

$$\begin{aligned} S_3'(t_r, t_a) &= S_3(t_r, t_a) \cdot exp\left\{-\frac{4\pi[R_{A_2J}(t_a) - R_{A_2J_1}(t_a)]}{\lambda}\right\} \\ &\quad * \delta\left\{t_r - \frac{2[R_{A_2J}(t_a) - R_{A_2J_1}(t_a)]}{c}\right\} \end{aligned} \tag{10}$$

where $\delta\{\cdot\}$ is the Dirac delta function. $R_{A_2J}(t_a)$ is the distance between the antenna A2 and the stationary jammer J varying t_a as follows.

$$\begin{aligned} R_{A_2J}(t_a) &= \sqrt{(vt_a - x_J)^2 + y_J^2 + h^2} \\ &\approx R_J - \frac{vx_1}{R_J}t_a + \frac{v^2t_a^2}{2R_J} \end{aligned} \tag{11}$$

where $R_J = \sqrt{x_J^2 + y_J^2 + h^2}$. Because both the jammer and the false target are usually located in the imaging area, the following approximation holds: $R_1 \approx R_J$.

After SAR processing [17], ignoring the same phase between the jamming images I_1 and I_3, the SAR image of false target J can be described as follows.

$$I_1(x_J, y_J) = I_J(x_J, y_J) \cdot \exp\left[-j\frac{2\pi D}{\lambda}\left(\frac{x_1}{R_1} - \frac{2x_J}{R_1}\right)\right] \tag{12}$$

$$I_3(x_J, y_J) = I_J(x_J, y_J) \cdot \exp\left[-j\frac{2\pi D}{\lambda}\left(-\frac{x_1}{R_1}\right)\right] \tag{13}$$

$$\begin{aligned} I_J(x_J, y_J) &= \sigma_J\left(1 - \frac{|t_a - x_J/v|}{T_a}\right)\left(1 - \frac{|t_r - t_J|}{T_r}\right) \\ &\quad \times \text{sinc}\left[\pi B_r(t_r - t_J)\left(1 - \frac{|t_r - t_J|}{T_r}\right)\right] \\ &\quad \times \text{sinc}\left[\pi B_a\left(t_a - \frac{x_J}{v}\right)\left(1 - \frac{|t_a - x_J/v|}{T_a}\right)\right] \end{aligned} \tag{14}$$

where $t_J = 2R_1/c$. Then, according to (12) and (13), the different phase of jamming image in different antenna is only relative to the jamming geometric model which contains the image position of jamming and the jammer in azimuth. The jamming image can be described after DPCA processing as follows.

$$\begin{aligned} I_{\text{DPCA}}(x_J, y_J) &= |I_3(x_J, y_J) - I_1(x_J, y_J)| \\ &= |I_J(x_J, y_J)| \cdot 2\left|\sin\left[\frac{2\pi D(x_J - x_1)}{\lambda R_1}\right]\right| \end{aligned} \tag{15}$$

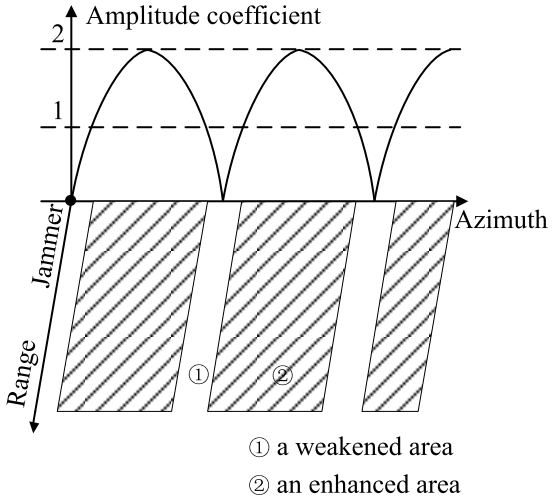

FIGURE 3. The azimuth jamming filter of DPCA image.

The SAR image is modulated by the amplitude coefficient related to the azimuth position of the jammer and the false target, and the maximum of the amplitude coefficient is 2. This process is likely that the SAR image is filtered by azimuth jamming filter as shown in the Fig.3. The jammer is at the order, and the jamming is suppressed by azimuth jamming filter related to the azimuth position of the jammer and the false target. Then, the jamming image has be classified as an enhanced area and a weakened area. In the weakened area, the jamming is suppressed by the azimuth jamming filter and $I_{\mathrm{DPCA}}(x_J, y_J) < |I_J(x_J, y_J)|$. In the enhanced area, the jamming is enhanced by the azimuth jamming filter and $I_{\mathrm{DPCA}}(x_J, y_J) \geq |I_J(x_J, y_J)|$.

In the enhanced area, the azimuth distance between the jammer and the jamming can be described as follows.

$$\frac{\lambda R_1(6k+1)}{12D} \leq x_J - x_1 \leq \frac{\lambda R_1(6k+5)}{12D} \tag{16}$$

where k is an integer. Correspondingly, in the weakened area, the distance between the jammer and the jamming can be described as follows.

$$\frac{\lambda R_1(6k-1)}{12D} < x_J - x_1 < \frac{\lambda R_1(6k+1)}{12D} \tag{17}$$

Although the jamming images are different, including barraged jamming method and deception jamming method, the jamming effect is relative to the azimuth position of the jammer and the jamming imaged in the SAR image. Jamming image will be suppressed or eliminated in the weakened area, and the information of the moving targets can be acquired by DPCA processing. So jamming method based on a single jammer cannot provide the effective protection in the whole imaging area.

III. PRINCIPLE OF BARRAGE NOISE JAMMING METHOD BASED ON DOUBLE JAMMERS

Based on the analysis of the jamming effect based on a single jammer in Section II, a barrage noise jamming method based on double jammers is proposed by changing the jamming geometric. By controlling the azimuth distance between the jammers, the suppression of SAR GMTI is destroyed, and the jamming can cover the whole DPCA image. As shown in Fig. 4, assume that there are two barrage noise jammers, J_1 and J_2, in the imaged area. Their coordinates are $(x_1, y_1, 0)$ and $(x_2, y_2, 0)$, respectively. The azimuth distance between J_1 and J_2 is Δx. According to Section II, the jamming image in two received antennas can be expressed, respectively, as

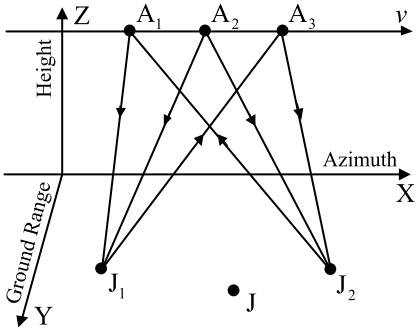

FIGURE 4. Geometric model of barrage noise jamming based on double jammers.

$$\begin{aligned} I_{\mathrm{A}_1}(x_J, y_J) = {} & I_{J1}(x_J, y_J) \cdot \exp\left[-\mathrm{j}\frac{2\pi}{\lambda}\left(\frac{x_1 D}{R_1} - \frac{2Dx_J}{R_1}\right)\right] \\ & + I_{J2}(x_J, y_J) \cdot \exp\left[-\mathrm{j}\frac{2\pi}{\lambda}\left(\frac{x_2 D}{R_2} - \frac{2Dx_J}{R_2}\right)\right] \end{aligned} \tag{18}$$

$$\begin{aligned} I_{\mathrm{A}_3}(x_J, y_J) = {} & I_{J1}(x_J, y_J) \cdot \exp\left[-\mathrm{j}\frac{2\pi}{\lambda}\left(-\frac{x_1 D}{R_1}\right)\right] \\ & + I_{J2}(x_J, y_J) \cdot \exp\left[-\mathrm{j}\frac{2\pi}{\lambda}\left(-\frac{x_2 D}{R_2}\right)\right] \end{aligned} \tag{19}$$

$$R_2 = \sqrt{x_2^2 + y_2^2 + h^2} \tag{20}$$

where $I_{J1}(x_J, y_J)$ and $I_{J2}(x_J, y_J)$ are barrage noise jamming images in the SAR image [17], and they are generated by jammers J_1 and J_2, respectively. The jamming image I_2 can be described by utilizing the jamming image I_1 as follows.

$$I_{J2}(x_J, y_J) = \mathrm{A} \cdot I_{J1}(x_J, y_J) \cdot \exp(\mathrm{j}\theta) \tag{21}$$

where A and θ are the amplitude and phase different between $I_{J1}(x_J, y_J)$ and $I_{J2}(x_J, y_J)$, respectively. The barrage noise jamming generated by two jammers are not need to coherent, and A and θ are Gaussian random variables.

After DPCA processing, the jamming image is as follows [21].

$$\begin{aligned} & I_{\mathrm{DPCA}}(x_J, y_J) \\ & = |I_{\mathrm{A}_3}(x_J, y_J) - I_{\mathrm{A}_1}(x_J, y_J)| \\ & = 2 \cdot \left[2\mathrm{A}\sin\left(\frac{\varphi_1}{2}\right)\sin\left(\frac{\varphi_2}{2}\right)\cos(\theta) \right. \\ & \quad \left. + \sin^2\left(\frac{\varphi_1}{2}\right) + \mathrm{A}^2\sin^2\left(\frac{\varphi_2}{2}\right)\right]^{1/2} \cdot |I_{J1}(x_J, y_J)| \end{aligned} \tag{22}$$

where

$$\varphi_1 = -\frac{4\pi D(x_1 - x_J)}{\lambda R_1} \tag{23}$$

$$\varphi_2 = -\frac{4\pi D(x_2 - x_J)}{\lambda R_2} \tag{24}$$

In order to generate noise in the whole DPCA image, $\varphi_2 = \varphi_1 + (1 + 4k)\pi/2$ should be obtained by controlling the azimuth distance between the two jammers where k is an integer, and the azimuth distance is shown as follows.

$$\Delta x = |x_2 - x_1| = \frac{(1 + 4k)\lambda R_1}{4D} \tag{25}$$

Then, (22) is simplified as follows.

$$I_{\mathrm{DPCA}}(x_J, y_J) = 2 \cdot \left[2\mathrm{A}\sin\left(\frac{\varphi_1}{2}\right)\cos\left(\frac{\varphi_1}{2}\right)\cos(\theta) + \sin^2\left(\frac{\varphi_1}{2}\right) + \mathrm{A}^2\cos^2\left(\frac{\varphi_1}{2}\right)\right]^{1/2} \cdot |I_{J1}(x_J, y_J)| \tag{26}$$

Considering the jammers are assumed have approximate jamming power, so the mean of A is approximately equal to 0 dB. In addition, because θ is Gaussian random variables, the mean of $\cos(\theta)$ is 0. Then, the mean amplitude of jamming image after DPCA processing can be described as follow.

$$\mathrm{E}[I_{\mathrm{DPCA}}(x_J, y_J)] = 2 \cdot |I_{J1}(x_J, y_J)| \tag{27}$$

So the proposed jamming method can generate the noise in the whole DPCA image, and the weakened area of jamming is avoided. In addition, the jamming amplitude gain is defined as the amplitude of the jamming in DPCA image and that generated based on the single jammer in SAR image ratio. According to (27), the mean of jamming amplitude gain generated with the proposed jamming method is 2. Meanwhile, according to (15), the maximum of jamming amplitude gain generated with the barrage noise jamming method based on a single jammer is 2. The proposed jamming method has the higher jamming amplitude gain while the noise can cover the whole DPCA image. So the proposed method is able to provide the effective protection in the whole DPCA image.

IV. SIMULATION RESULTS

In this section, simulation result of barrage noise jamming based on double jammers against SAR GMTI compared with that of barrage noise jamming based on a single jammer.

A. SIMULATION PARAMETERS OF SAR GMTI

The azimuth and ground range length of the illumined area are 300 m and 100 m, respectively. The primary parameters of the SAR GMTI are listed in TABLE 1.

The area without jamming is imaged and shown in Fig. 5. These are set for contrast and further analysis, and moving targets are imaged and pointed. The Signal Noise Ratio (SNR) is assumed as 13.2 dB where detection probability is 0.9 and false-alarm probability is 10^{-6}, and the Clutter Noise Ratio (CNR) is assumed as 20 dB [22].

TABLE 1. Simulation parameter.

Parameters	Symbol	Value
SAR velocity	v	200 m/s
Pulse repetition frequency	PRF	1024 Hz
Effective baseline	D	3.125 m
Altitude	h	5,000 m
Pulse duration	T_r	20 μs
Signal bandwidth	B_r	200 MHz
Target exposure time	T_a	0.88 s
Radar center frequency	f_0	9.6 GHz

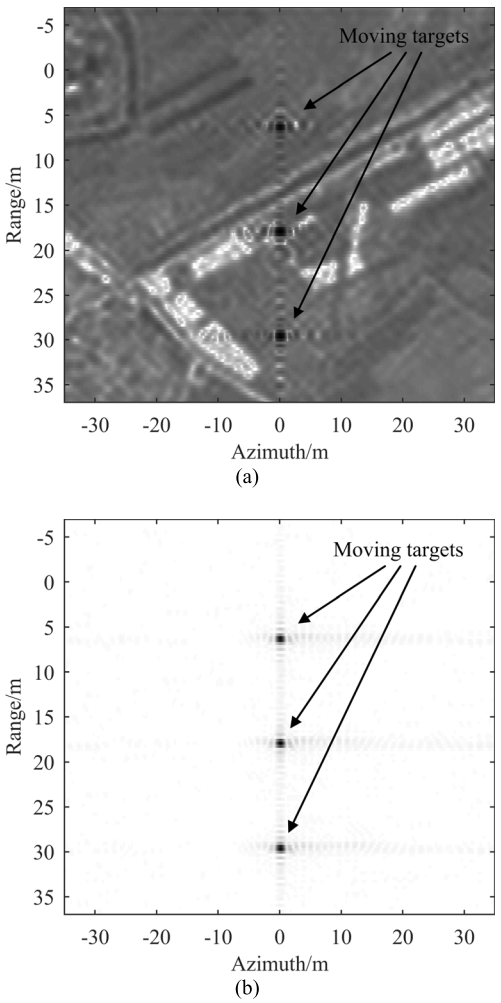

FIGURE 5. SAR and DPCA images without jamming. (a) SAR image. (b) DPCA image.

B. BARRAGE NOISE JAMMING BASED ON A SINGLE JAMMER

The barrage noise jamming result based on a single jammer is set for contrast analysis. The coordinate of a single jammer is (0 m, 10000 m, 0 m). The Jamming Signal Ratio (JSR) is 30 dB. The results of SAR and DPCA images are shown in Fig 6. (a) and (b). In addition, azimuth sectional plots of SAR and DPCA images are present in Fig 6. (c) and (d), and the amplitude of jamming is normalized by using the maximum amplitude of the jamming in the SAR image.

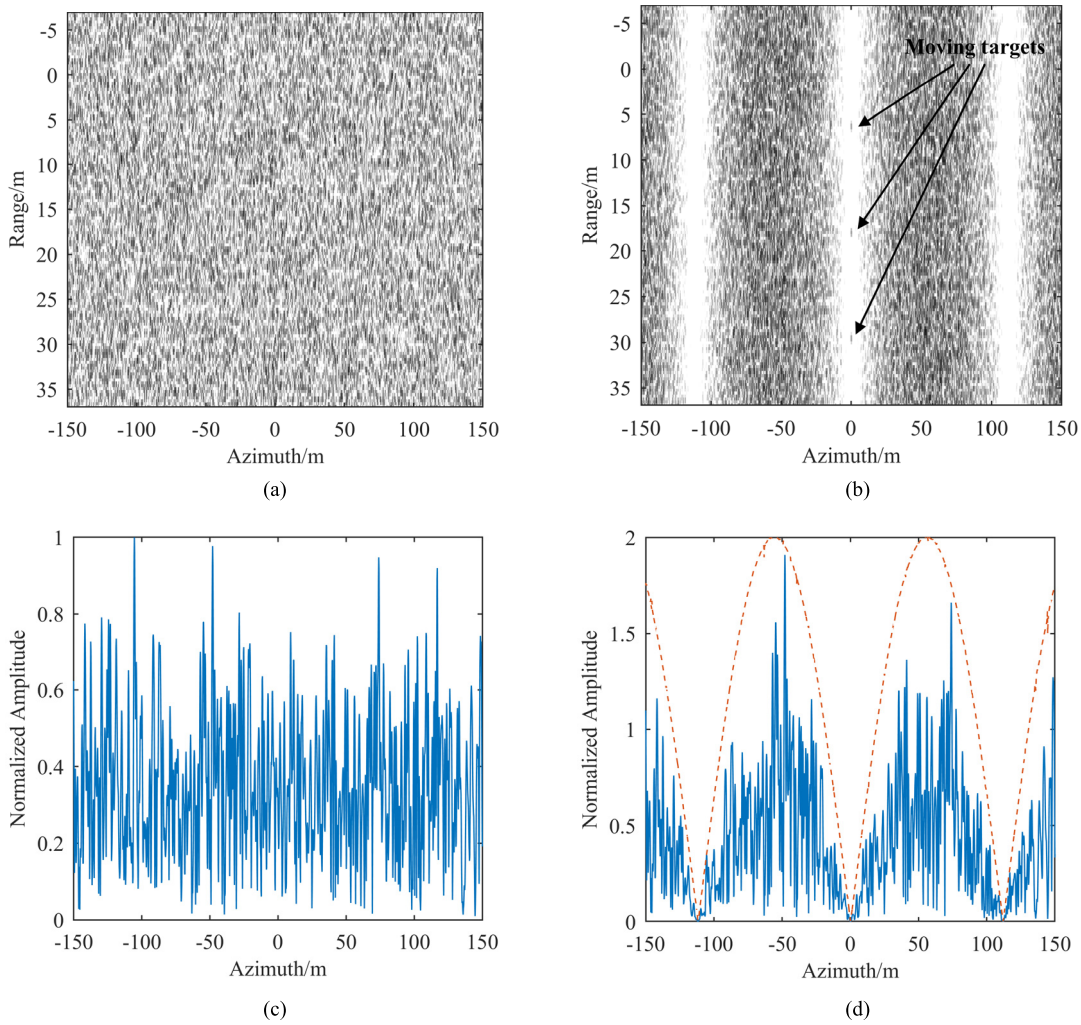

FIGURE 6. SAR and DPCA images with barrage noise jamming based on a single jammer. (a) SAR image. (b) DPCA image. (c) azimuth sectional plot of SAR image. (d) azimuth sectional plot of DPCA image.

As shown in Fig. 6. (a) and (c), the barrage noise jamming based on the signal jammer can cover the whole imaging area, but jamming in the DPCA image will be suppressed as shown in Fig. 6. (b) and (d), and moving targets are imaged and detected in DPCA image. In addition, the dashed line presents the amplitude coefficient of the azimuth jamming filter as shown in Fig, 6 (d), and it satisfied(15). So barrage noise jamming method based on a single jammer cannot provide the effective protection in the whole imaging area.

C. FALSE TARGETS DECEPTION JAMMING

False moving targets deception jamming method is an important deception jamming method, and it is proved as the effective jamming method against SAR GMTI [15], [16]. The intercepted radar signal is modulated by range time-delay and phase modulation to form the echo of false moving targets. In order to show the advantages of the proposed method, the jamming result is set for contrast analysis.

The coordinate of a single jammer is (0 m, 10000 m, 0 m). Four false moving target are generated in the illuminated area. The velocity of the false moving targets is shown in Table 2. The JSR is 0 dB. The SAR and DPCA results are shown in Fig 7. (a) and (b). In addition, azimuth sectional plots of SAR and DPCA images are present in Fig 7. (c) and (d), and the amplitude of jamming is normalized by using the maximum amplitude of the jamming in the SAR image.

As shown in Fig.7. (a) and (c), the false targets are generated beside the real moving targets, and the targets have the same amplitude. So false moving targets deception jamming can prove the effective protection in SAR image. However, as shown in Fig.7. (b) and (d), the false moving targets deception jamming will be suppressed by the azimuth jamming filter. The dashed line presents the amplitude coefficient of the azimuth jamming filter as shown in Fig, 7 (d), and it satisfied(15). Then, the analysis of reason why the jamming based on a single jammer is eliminated in Section II is verified. So, we can draw a conclusion from Section IV B. and C. : the

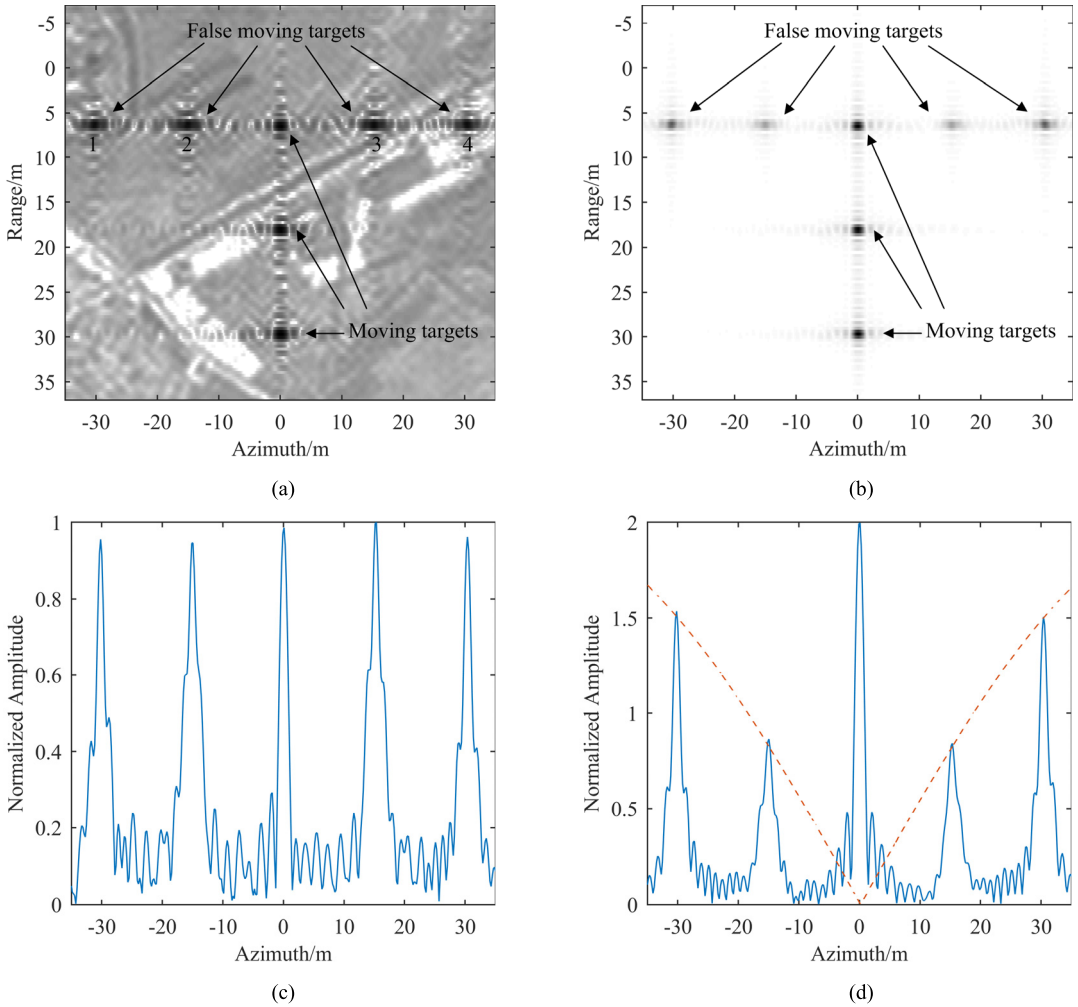

FIGURE 7. SAR and DPCA images with false targets deception jamming. (a) SAR image. (b) DPCA image. (c) azimuth sectional plot of SAR image. (d) azimuth sectional plot of DPCA image.

TABLE 2. The velocity of four false moving targets.

Serial	Azimuth velocity	Ground range velocity
1	2 m/s	0.6 m/s
2	2 m/s	0.3 m/s
3	2 m/s	-0.3 m/s
4	2 m/s	-0.6 m/s

jamming method based on a single jammer cannot provide the effective protection in whole imaging area.

D. BARRAGE NOISE JAMMING BASED ON DOUBLE JAMMERS

According to (25), the coordinates of two jammers J1 and J2 are (0 m, 10000 m, 0 m) and (28 m, 10000 m, 0 m), respectively. JSR is 30 dB. The jamming result is imaged as shown in Fig. 8. The SAR and DPCA results are shown in Fig 8. (a) and (b). In addition, azimuth sectional plots of SAR and DPCA images are present in Fig 8. (c) and (d), and the amplitude of jamming based on double jammers is normalized by using the maximum amplitude of the jamming in the SAR image.

As shown in Fig 8. (a) and (c), jamming based on double jammers can cover the whole SAR image. In addition, the jamming based on double jammers can be generated in the whole image area and moving targets cannot be effectively detected form SAR image after DPCA processing as shown in Fig 8. (b) and (d), and the mean of jamming amplitude gain is 2.02, which jamming amplitude gain is defined as the amplitude of the jamming in DPCA image and that generated based on the single jammer in SAR image ratio in Section III. In Section III, according to (27), the mean of jamming amplitude gain generated with the proposed jamming method is 2 in theory. The result of theory and experience are nearly same.

In addition, the result of jamming amplitude gain after 1000 experiments is shown as Fig. 9. The mean of the result is 2.01. The jamming amplitude gain error between simulation and theory is 0.01, and it is too slight to notice, which verifies the effectiveness of the proposed algorithm. So the proposed

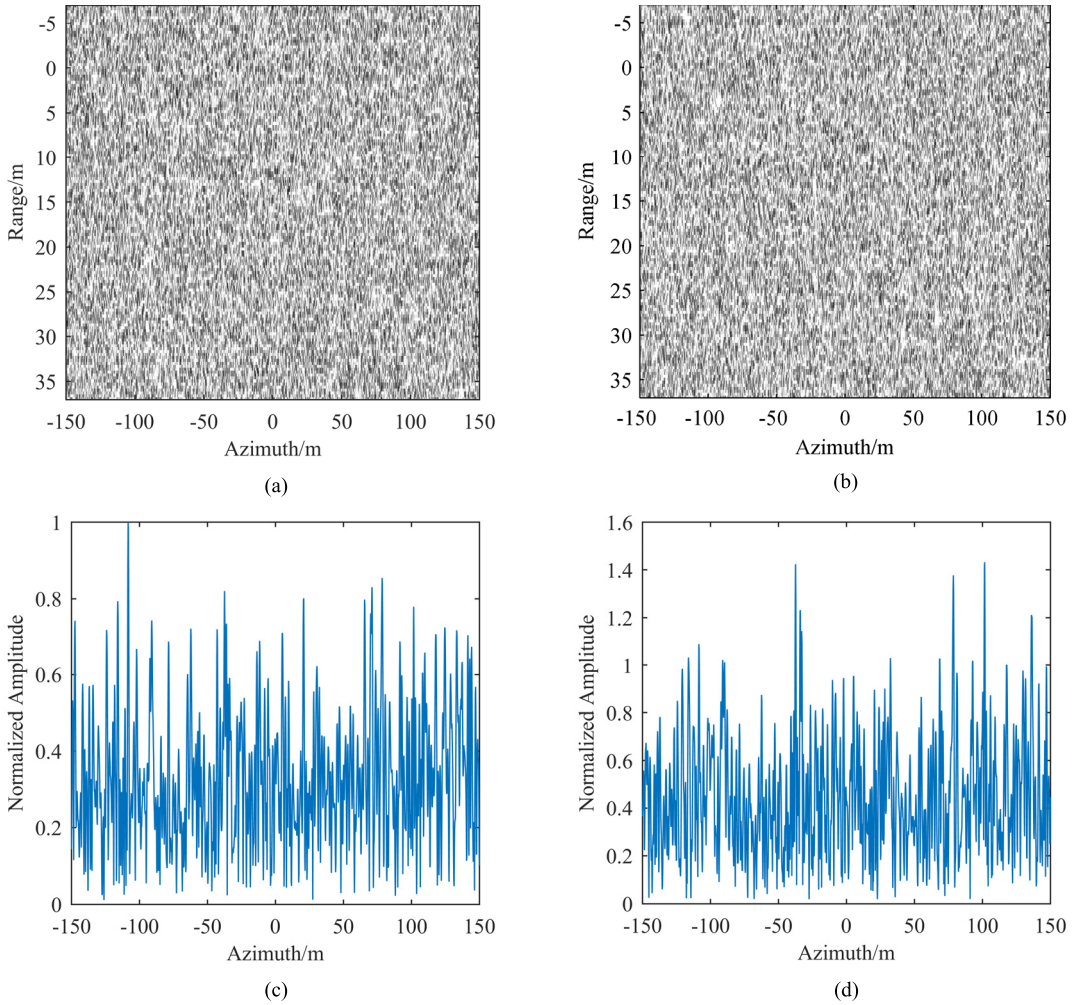

FIGURE 8. SAR and DPCA images with barrage noise jamming based on double jammers. (a) SAR image. (b) DPCA image. (c) azimuth sectional plot of SAR image. (d) azimuth sectional plot of DPCA image.

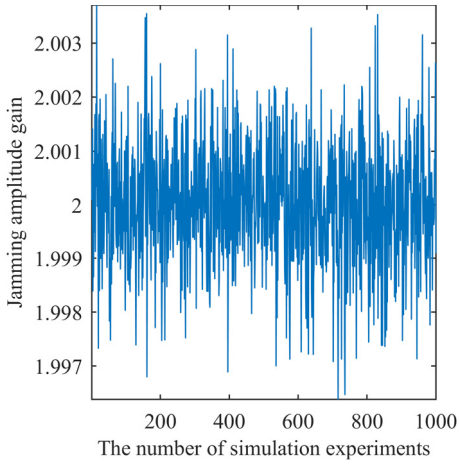

FIGURE 9. Result of the gain coefficient after 1000 experiments.

method is able to prove the effective protection in the whole DPCA image.

V. CONCLUSION

Two important problems faced by the jammer are why the jamming based on a single jammer is suppressed or eliminated and how to generate noise in the whole DPCA image. By analyzing jamming geometric model based on a single jammer, the reason is that the phase of jamming image in different antenna is only relative to the jamming geometric model which contains the azimuth position of the jammer and jamming in SAR image. By analyzing the jamming effect based on a single jammer, the azimuth jamming filter is used to explain that jamming will be suppressed after DPCA processing. The jamming area will be classified as an enhanced area and a weakened area. In the weakened area, jamming cannot cover real moving targets, so information of moving targets are detected. To overcome this disadvantage, a barrage noise jamming method based on double jammers is proposed. By controlling the distance between double jammers, the phase of jamming signal in the two received antennas can be changed, and the suppression of SAR GMTI will be destroyed. The whole SAR and GMTI images are covered by noise, and the information of moving targets cannot be detected by utilizing DPCA processing. Compared with the deception jamming method based on multiple coherent jammers, the phase and amplitude of jamming signal are not need to be accurately controlled. In addition, the jamming energy

of the proposed jamming is more than that of a barrage noise jamming based the single jammer while keeping its easy realization. The validity is verified by simulation experiments.

REFERENCES

[1] F. Gao, F. Ma, J. Wang, J. Sun, E. Yang, and H. Zhou, "Visual saliency modeling for river detection in high-resolution SAR imagery," *IEEE Access*, vol. 6, pp. 1000–1014, Nov. 2017.

[2] W. Lv, K. Dai, L. Wu, X. Yang, and W. Xu, "Runway detection in SAR images based on fusion sparse representation and semantic spatial matching," *IEEE Access*, vol. 6, pp. 27984–27992, May 2018.

[3] S. Chiu and C. Livingstone, "A comparison of displaced phase centre antenna and along-track interferometry techniques for RADARSAT-2 ground moving target indication," *Can. J. Remote Sens.*, vol. 31, no. 1, pp. 37–51, Feb. 2005.

[4] S. Tanelli, S. L. Durden, and M. P. Johnson, "Airborne demonstration of DPCA for velocity measurements of distributed targets," *IEEE Geosci. Remote Sens. Lett.*, vol. 13, no. 10, pp. 1415–1419, Oct. 2016.

[5] K. Suwa, K. Yamamoto, M. Tsuchida, S. Nakamura, T. Wakayama, and T. Hara, "Image-based target detection and radial velocity estimation methods for multichannel SAR-GMTI," *IEEE Trans. Geosci. Remote Sens.*, vol. 55, no. 3, pp. 1325–1338, Mar. 2017.

[6] B. Zhao, F. Zhou, M. L. Tao, Z. J. Zhang, and Z. Bao, "Improved method for synthetic aperture radar scattered wave deception jamming," *IET Radar, Sonar Navigat.*, vol. 8, no. 8, pp. 971–976, Oct. 2014.

[7] M. Fang, D. Bi, and A. Shen, "Countering performance analysis of scatter-wave jamming against multi-channel SAR-GMTI," in *Proc. CIE Int. Conf. Radar (RADAR)*, Suzhou, China, Oct. 2016, pp. 1–5.

[8] L. Jia, X. Jia, Y. He, and C. Huang, "Analysis on the effects of rebound jamming on InSAR imaging," *Electron. Warfare Technol.*, vol. 27, no. 3, pp. 42–48, May 2012.

[9] L. Huang, C. Dong, Z. Shen, and G. Zhao, "The influence of rebound jamming on SAR GMTI," *IEEE Geosci. Remote Sens. Lett.*, vol. 12, no. 2, pp. 399–403, Feb. 2015.

[10] C. Dong and X. Chang, "A novel scattered wave deception jamming against three channel SAR GMTI," *IEEE Access*, vol. 6, pp. 53882–53889, Dec. 2018.

[11] B. Zhao, L. Huang, J. Li, M. Liu, and J. Wang, "Deceptive SAR jamming based on 1-bit sampling and time-varying thresholds," *IEEE J. Sel. Topics Appl. Earth Observ. Remote Sens.*, vol. 11, no. 3, pp. 939–950, Mar. 2018.

[12] F. Zhou, B. Zhao, M. Tao, X. Bai, B. Chen, and G. Sun, "A large scene deceptive jamming method for space-borne SAR," *IEEE Trans. Geosci. Remote Sens.*, vol. 51, no. 8, pp. 4486–4495, Aug. 2013.

[13] B. Zhao, F. Zhou, and Z. Bao, "Deception jamming for squint SAR based on multiple receivers," *IEEE J. Sel. Topics Appl. Earth Observ. Remote Sens.*, vol. 8, no. 8, pp. 3988–3998, Aug. 2015.

[14] X.-R. Shi, F. Zhou, B. Zhao, M.-L. Tao, and Z.-J. Zhang, "Deception jamming method based on micro-Doppler effect for vehicle target," *IET Radar, Sonar Navigat.*, vol. 10, no. 6, pp. 1071–1079, Jul. 2016.

[15] J. Zhang, D. Dai, Z. Qi, Y. Zeng, and S. Xiao, "Analysis of deceptive moving target generated by single jammer in multi-channel SAR-GMTI," in *Proc. Int. Appl. Comput. Electromagn. Soc. Symp. (ACES)*, Suzhou, China, Aug. 2017, pp. 1–2.

[16] J. Zhang, D. Dai, S. Xing, S. Xiao, and B. Pang, "A novel barrage repeater jamming against SAR-GMTI," in *Proc. 10th Eur. Conf. Antennas Propag. (EuCAP)*, Davos, Switzerland, Apr. 2016, pp. 1–5.

[17] F. Zhou, G. Sun, X. Bai, and Z. Bao, "A novel method for adaptive SAR barrage jamming suppression," *IEEE Geosci. Remote Sens. Lett.*, vol. 9, no. 2, pp. 292–296, Mar. 2012.

[18] L. Hong, C. X. Dong, and G. Q. Zhao, "Investigation on countermeasure against SAR dual-channel cancellation technique with multi-jammers," *J. Electron. Inf. Technol.*, vol. 36, no. 4, pp. 904–907, Apr. 2014.

[19] H. Xu, Z. Wu, W. Liu, J. Li, and Q. Feng, "Analysis of the effect of interference on InSAR," *IEEE Sensors J.*, vol. 15, no. 10, pp. 5659–5668, Oct. 2015.

[20] J. Zhang, S. Xing, D. Dai, Y. Li, and S. Xiao, "Three-dimensional deceptive scene generation against single-pass InSAR based on coherent transponders," *IET Radar, Sonar Navigat.*, vol. 10, no. 3, pp. 477–487, Mar. 2016.

[21] J. Zhang, "Study on distributed cooperative jamming techniques against multichannel SAR," Ph.D. dissertation, Dept. Inf. Commun. Eng., Nat. Univ. Defense Technol., Changsha, Hunan, China, 2016.

[22] Z.-F. Wu, H.-P. Xu, J.-W. Li, and W. Liu, "Research of 3-D deceptive interfering method for single-pass spaceborne InSAR," *IEEE Trans. Aerosp. Electron. Syst.*, vol. 51, no. 4, pp. 2834–2846, Oct. 2015.

[23] D. K. Barton, *Radar System Analysis and Modeling*. Norwood, MA, USA: Artech House, 2005.

XIN CHANG was born in Shijiazhuang, Hebei, China, in 1990. He received the M.E. degree from Xidian University, Xi'an, China, in 2017, where he is currently pursuing the Ph.D. degree with the School of Electronic Engineering. His main research interests include ECM technology and EW system simulation.

CHUNXI DONG was born in Henan, China, in 1970. He received the Ph.D. degree from Xidian University, Xi'an, China, in 2004, where he is currently an Associate Professor with the School of Electronic Engineering. His main research interests include ECM technology and EW system simulation.